

# Macromolecules

Volume 38, Number 17

August 23, 2005

© Copyright 2005 by the American Chemical Society

## Communications to the Editor

### Real-Time Neutron Scattering Study of Transient Phases in Polymer Crystallization

Xiangbing Zeng,<sup>\*,†</sup> Goran Ungar,<sup>‡</sup>  
Stephen J. Spells,<sup>§</sup> and Stephen M. King<sup>§</sup>

*Department of Engineering Materials, University of Sheffield, Sheffield S1 3JD, UK; Sheffield Hallam University, City Campus, Sheffield S1 1WB, UK; and ISIS, Rutherford Appleton Laboratory, Chilton, Didcot OX11 0QX, UK*

*Received May 23, 2005*

*Revised Manuscript Received June 27, 2005*

Crystallizable polymers form thin (10–50 nm) crystalline lamellae through chain folding. Some of the most powerful techniques for studying such lamellar structures are small-angle neutron and X-ray scattering (SANS and SAXS). SANS has been used successfully for mapping the overall shape of deuterated macromolecules in a hydrogenous host environment, thus providing answers to questions relating to the “reeling in” of chains on crystallization<sup>1,2</sup> and the adjacency of chain folding.<sup>3</sup> For molecules with selectively deuterated segments, SANS is able to provide information on the location and state of order of such segments. The complementarity of SAXS and SANS has been demonstrated, e.g., in recent investigations of the stable semicrystalline form and the low-temperature triple-layer crystalline superlattice phase in binary mixtures of very long linear alkanes.<sup>4,5</sup>

Polymer crystallization is a highly nonequilibrium process,<sup>6</sup> and it is often accompanied by the appearance of transient forms and solid-state transformations.<sup>7</sup> For some time now, it has been demonstrated that SAXS data with a reasonable signal-to-noise ratio can be collected in subsecond frames (time slices) using synchrotron radiation sources. This makes real-time SAXS

suitable for studies of the crystallization process in polymers and other materials.<sup>8</sup> It would be ideal if similar real-time experiments could be carried out with SANS to supplement the information obtained by SAXS. However, SANS data of a similar signal-to-noise ratio normally take hours to collect, even at the most powerful neutron sources available. Consequently, relatively few SANS experiments on second time scales have been carried out.<sup>9–14</sup> Time-resolved SANS study of polyethylene crystallization from solution has been carried out recently, but on a larger time scale.<sup>15</sup>

One example where such studies may provide more direct information than SAXS is resolving the structure of the transient “noninteger folded” form (NIF) in pure long chain linear alkanes. These model polymers, containing between 150 and 400 C atoms, crystallize in layers with the chains either fully extended or folded exactly in two, three, etc.<sup>16</sup> In such “integer forms” chain ends are segregated at the crystal surface. However, real-time SAXS experiments revealed that during melt-crystallization such structures are mostly produced via a transient NIF form, where layer periodicity does not correspond to an integer fraction of the extended chain length.<sup>17</sup> Integer folded forms, such as extended, once folded, or the triple-layer mixed folded-extended form<sup>18</sup> (Figure 1a–c), develop subsequently through solid-state transformation. It is believed that the formation of NIF and its subsequent transformation to more stable forms is a good model for the technologically important processes of primary and secondary crystallization of polymers.

On the basis of Fourier reconstruction of the electron density profile from the real-time SAXS data, a structural model for NIF has been proposed (model I, Figure 1d).<sup>19</sup> In the model some molecules are folded exactly in two while others are not folded, traversing the crystal layer only once and leaving their dangling ends to form an interlamellar amorphous layer. However, in another popular model of NIF, proposed initially for alkanes<sup>17</sup> and subsequently for poly(ethylene oxide),<sup>20</sup> molecules fold irregularly, having their ends distributed through-

<sup>†</sup> University of Sheffield.

<sup>‡</sup> Sheffield Hallam University.

<sup>§</sup> Rutherford Appleton Laboratory.

\* Corresponding author: e-mail x.zeng@sheffield.ac.uk.

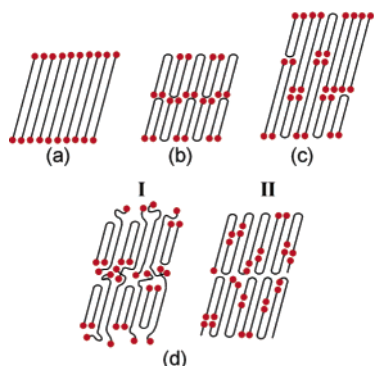


**Figure 1.** Schematic drawings of different lamellar structures of the end-deuterated long-chain alkane  $C_{12}D_{25}C_{192}H_{384}CHDC_{11}D_{23}$  during isothermal crystallization. (a) Extended chain form. (b) Once-folded chain form. (c) Triple-layer mixed folded-extended (FE) form. (d) Alternative models for the noninteger folded (NIF) form. With the help of deuterium labels, shown as red circles, real-time SANS is able to monitor the location of the chain ends during the crystallization process.

out the crystal layer (model II, Figure 1d). SANS on the deuterium end-labeled molecules is an ideal method for distinguishing between the two models of NIF, as the latter model would produce very weak, if any, scattering. The material chosen in the current study is  $C_{12}D_{25}C_{192}H_{384}CHDC_{11}D_{23}$  (abbreviated C216D), synthesized by Dr. Brooke at Durham University.<sup>21</sup> Since only the hydrogen atoms in the last 12  $CH_2$  groups at both ends of a  $C_{216}H_{385}D_{49}$  molecule were deuterated, no microphase separation between  $CD_2$  and  $CH_2$  is expected in the melt.

Because of the short lifetime of the NIF form (less than a minute for C216D), SANS with comparable time resolution is needed. Our recent experiments on C216D have shown that as a consequence of the selective deuteration SANS spectra with reasonable signal-noise ratio can be collected in a few seconds.

The experiments were carried out on the LOQ diffractometer at the ISIS Spallation Neutron Source at the Rutherford-Appleton Laboratory, UK. A technical prerequisite for fast time-resolved experiments is the ability to cool a relatively large amount of sample ( $\sim 100$  mg) rapidly and homogeneously from the melt to the crystallization temperature. For this purpose modifications were made to the temperature-jump cell previously used in ref 22. The sample, held in an aluminum cuvette of uniform 1 mm cavity thickness, could be quickly transferred (of order 1 s) by a motorized slider between two electrically heated furnaces at preset temperatures, with a spring-loaded window assembly ensuring the instant establishment of good thermal contact over the entire area of the cuvette (Figure 2). The transfer of the sample to the in-beam furnace was synchronized with the start of the SANS data collection, and the data acquisition memory was subdivided into a maximum of 39 contiguous frames. There was no "dead time" between frames, and the length of each frame could be varied as necessary. Signal-to-noise limitations, however, imposed a minimum data collection time of 5 s/frame.

Isothermal crystallization experiments on C216D using real-time SANS were carried out at four different temperatures: 121, 115, 107, and 102 °C. For each experimental run the sample was first melted in the out-of-beam furnace set at 134 °C and then transferred to

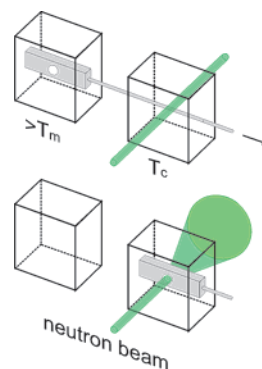


**Figure 2.** Schematic drawing of the T-jump cell used for the real-time SANS experiment.

the in-beam furnace set at the predetermined crystallization temperature  $T_c$ . For reference, the melting point of C216D is  $T_m = 127$  °C, as determined by XRD, optical microscopy, and DSC. The SANS spectra are shown in Figure 3a–d for each temperature. The data have been corrected for the scattering of the empty furnace, sample absorption, and sample volume and have been converted to an absolute scale by reference to the scattering of a standard scatterer using established procedures.

At the highest crystallization temperature of 121 °C, C216D crystallizes in the extended chain form directly from the melt. The first four diffraction orders of the extended-chain lamellar stacks are evident in Figure 3a, and their positions do not change with time. The advance of crystallization is reflected in the increasing diffraction intensity with time in the first 3 min. The lamellar thickness is determined from SANS to be 230 Å, very close to the calculated value of 227 Å assuming that chains are extended and tilted at 35° with respect to lamellar normal, as expected from the usual {201} basal surface.

At  $T_c = 115$  °C the SANS spectra clearly show that crystallization starts in the NIF form, which then, within a couple of minutes, transforms to other more stable forms (Figure 3b). The crystallization rate of NIF at 115 °C is much faster than that of the extended chain form at 121 °C, and detectable crystallization had already started in the first frame. The measured lamellar thickness of the NIF form is 184 Å, i.e., intermediate between those of the extended (227 Å) and the once-folded (114 Å) forms. The mere fact that a NIF peak of significant intensity is observed in SANS at all implies that the model of the NIF form in which chain ends are distributed through the depth of the crystal layer (model II, Figure 1) can be dismissed in alkanes. Furthermore, the fact that only the first-order NIF peak is of sufficient intensity to be observed agrees with the structural model proposed previously on the basis of real-time SAXS experiments. According to the model the chain ends, i.e., the strongly scattering deuterium labels, are located only in the amorphous layers and at the crystalline–amorphous interface. Thus, the scattering length profile oscillates between high and low along the layer normal. The first diffraction order of such a structure is expected to be dominant.

The more stable lamellar structure into which the NIF form transforms on annealing at 115 °C (Figure 3b) is believed to consist of both extended and once-folded chains.<sup>17,23</sup> Four diffraction peaks are observed by SANS, and their positions are the same as those of the extended chain form observed at 121 °C. The

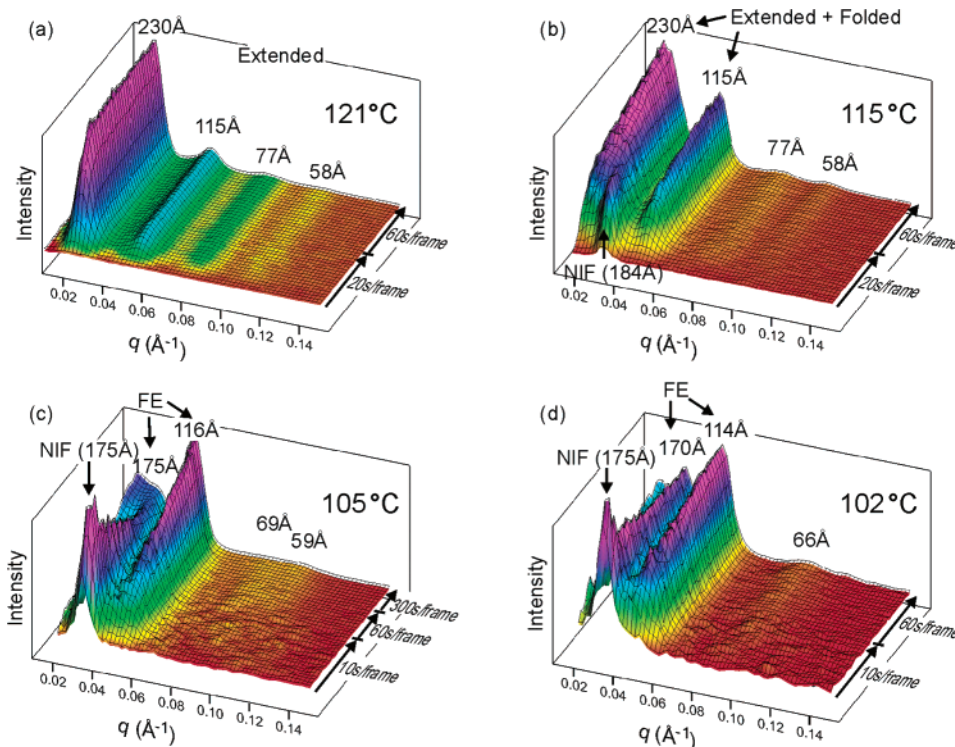


**Figure 3.** Real-time SANS spectra of  $C_{12}D_{26}C_{192}H_{384}CHDC_{11}D_{23}$  during isothermal crystallization at (a) 121, (b) 115, (c) 107, and (d) 102 °C. The peaks are marked by their  $2\pi/q$  values.

existence of the once-folded form in the sample is identified by the increased relative intensities of the second and fourth diffraction peaks. Recent AFM studies suggest that the folded chains may be incorporated in, rather than segregated out of, the extended-chain layers.<sup>23</sup>

At the next lower crystallization temperature of 107 °C (Figure 3c), C216D also crystallizes in the transient NIF form first, but it then undergoes a rapid solid-state transformation and disappears within about a minute. As expected, the crystallization rate of the NIF form is faster than at 115 °C. Here the lamellar thickness of the NIF form is found to be 175 Å.

The phase that the NIF form converts into at 107 °C is characterized by four diffraction peaks with spacings corresponding to 175, 116, 69 (weak), and 59 Å (weak) (Figure 3c). The 175 Å peak coincides with the main peak of the precursor NIF form. The intensity ratio of the four reflections of the new form changes gradually with time, the 175 Å peak giving way to that at 116 Å. The four diffraction peaks can be indexed as the second, third, fifth, and sixth orders of a single lamellar periodicity of  $\sim 350$  Å. This is believed to represent the folded-extended (FE) form in which folded-chain and extended-chain molecules coexist in a triple-layer superlattice arrangement, as shown in Figure 1c. The folded-extended form was originally found by real-time SAXS and Raman spectroscopy in a hydrogenous *n*-alkane of similar length,  $C_{210}H_{422}$ .<sup>18</sup> Recent real-time SAXS experiments on the same deuterated C216D compound have also indicated the existence of the FE form under similar crystallization conditions. SAXS and SANS spectra of the FE form of C216D are displayed together in Figure 4. The SANS spectrum was recorded soon after the completion of the time-resolved run in Figure 3c. The observed intensity distribution between diffraction peaks in SANS is in accordance with the triple-layer superlattice model and is the first SANS

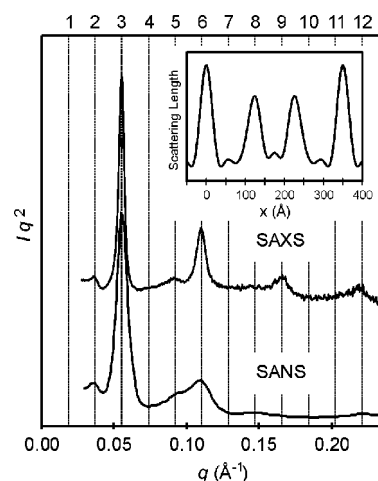


**Figure 4.** SAXS and SANS spectra of the FE form of C216D. In both cases the sample was isothermally crystallized at 107 °C, and the spectra were taken at the same temperature. Both spectra are Lorentz corrected. Vertical lines are drawn to indicate the order of the observed diffraction peaks. Inset: scattering length profile reconstructed from the SANS spectra showing the triple-layer superlattice structure of the FE form. The peaks in the profile indicate the positions of the deuterated chain ends.

confirmation of the FE form in long chain *n*-alkanes. This is shown more clearly in the neutron scattering length profile of the FE form (Figure 4, inset), reconstructed from the measured intensities of diffraction peaks in the SANS spectrum. For details of the reconstruction procedure see refs 4 and 5. The continuous change in relative diffraction intensity of different orders, particularly prominent in Figure 3c, shows that the distribution of chain ends among the three interfaces of the triple layer (Figure 1c) becomes more uniform. That is, the difference between the high population at the outer surfaces and the low population



at inner surfaces diminishes. The details are currently being investigated.

At the lowest crystallization temperature of 102 °C, C216D crystallizes again as the NIF form (lamellar thickness 175 Å) and then transforms to the FE form with lamellar thickness of ~340 Å. Three orders are observed: second, 170 Å third, 114 Å fifth, 66 Å (Figure 3d). The transition from the NIF form to the FE form occurs even faster than at 107 °C; i.e., it is complete within ca. 40 s. Finally, we note that at the end of the run at 107 °C a broad background develops at the lowest  $q$  end of the SANS spectrum (Figure 3c), a feature which is much less prominent at 102 °C. One possible explanation is the formation of extra extended chain layers produced by lamellar thickening at 107 °C.

In conclusion, it has been demonstrated that good quality SANS data can be collected in no more than 10 s for a model polymer system, provided a rational approach is adopted to selective deuteration. This points to a new way of using neutron scattering in studies of materials under rapid processing conditions.

**Acknowledgment.** We are indebted to Dr. G. M. Brooke for the preparation of the deuterated long alkane and to A. Gleeson of Daresbury Synchrotron Radiation Source for assistance with SAXS experiments. We thank CCLRC for providing beamtime at Daresbury SRS and ISIS and Prof. J. S. Higgins of Imperial College for allowing us to use the T-jump cell.

## References and Notes

- (1) Sadler, D. M.; Keller, A. *Macromolecules* **1977**, *10*, 1128–1140.
- (2) Dettenmaier, M.; Fischer, E. W.; Stamm, M. *Colloid Polym. Sci.* **1980**, *258*, 343–349.
- (3) Spells, S. J. In *Characterization of Solid Polymers*; Spells, S. J., Ed.; Chapman and Hall: London, 1994.
- (4) Zeng, X. B.; Ungar, G.; Spells, S. J.; Brooke, G. M.; Farren, C.; Harden, A. *Phys. Rev. Lett.* **2003**, *90*, 155508.
- (5) Zeng, X. B.; Ungar, G. *Macromolecules* **2003**, *36*, 4686–4688.
- (6) Wunderlich, B. *Macromolecular Physics*; Academic Press: New York, 1973, Vol. 1; 1976, Vol. 2.
- (7) Martinezsalazar, J.; Barham, P. J.; Keller, A. *J. Mater. Sci.* **1985**, *20*, 1616–1624.
- (8) Ungar, G. X-ray studies using synchrotron radiation. In *Characterization of Solid Polymers*; Spells, S. J., Ed.; Chapman and Hall: London, 1994; pp 56–121.
- (9) Porcar, L.; Hamilton, W. A.; Butler, P. D.; Warr, G. G. *Phys. Rev. Lett.* **2004**, *93*, 198301.
- (10) Nawroth, T.; Rusp, M.; May, R. P. *Physica B* **2004**, *350*, 635–638.
- (11) Grillo, I.; Kats, E. I.; Muratov, A. R. *Langmuir* **2003**, *19*, 4573–4581.
- (12) Simmons, B.; Agarwal, V.; Singh, M.; McPherson, G.; John, V.; Bose, A. *Langmuir* **2003**, *19*, 6329–6332.
- (13) Barreleiro, P. C. A.; May, R. P.; Lindman, B. *Faraday Discuss.* **2002**, *122*, 191–201.
- (14) Schwahn, D.; Janssen, S.; Springer, T. *J. Chem. Phys.* **1992**, *97*, 8775–8788.
- (15) Wang, H. *J. Polym. Sci., Part B: Polym. Phys.* **2004**, *42*, 3133–3147.
- (16) Ungar, G.; Stejny, J.; Keller, A.; Bidd, I.; Whiting, M. C. *Science* **1985**, *229*, 386–389.
- (17) Ungar, G.; Keller, A. *Polymer* **1986**, *27*, 1835–1844.
- (18) Ungar, G.; Zeng, X. B.; Spells, S. J. *Polymer* **2000**, *41*, 8775–8780.
- (19) Zeng, X. B.; Ungar, G. *Polymer* **1998**, *39*, 4523–4533.
- (20) Cheng, S. Z. D.; Chen, J. H.; Zhang, A. Q.; Barley, J. S.; Habenschuss, A.; Schack, P. R. *Polymer* **1992**, *33*, 1140–1149.
- (21) Brooke, G. M.; Farren, C.; Harden, A.; Whiting, M. C. *Polymer* **2001**, *42*, 2777–2784.
- (22) Cabral, J. T.; Gerard, H.; Clarke, N.; Higgins, J. S. *Physica B* **2000**, *276*, 408–409.
- (23) Tracz, A.; Ungar, G. *Macromolecules* **2005**, *38*, 4962–4965.

MA0510486